Since January 2020 Elsevier has created a COVID-19 resource centre with free information in English and Mandarin on the novel coronavirus COVID-19. The COVID-19 resource centre is hosted on Elsevier Connect, the company's public news and information website.

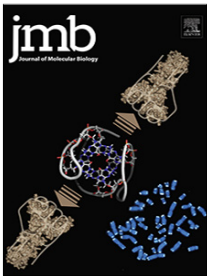

Structure-based Design of a Specific, Homogeneous Luminescence Enzyme Reporter Assay for SARS-CoV-2

Frederic A. Fellouse [1,2*], Shane Miersch [1,2], Chao Chen [1,2] and Stephen W. Michnick [3*]

*1 - **The Donnelly Centre,** University of Toronto, Toronto, Canada*
*2 - **Department of Molecular Genetics,** University of Toronto, Toronto, Canada*
*3 - **Département de Biochimie,** Université de Montréal, Montréal, Canada*

Correspondence to Frederic A. Fellouse and Stephen W. Michnick: Corresponding authors at: Département de biochimie, Université de Montréal, Montréal, Canada (S. W. Michnick) and The Donnelly Centre, University of Toronto, Toronto, Canada (F. A. Fellouse). *fred.fellouse@utoronto.ca (F. A. Fellouse), stephen.michnick@umontreal.ca (S. W. Michnick)*
https://doi.org/10.1016/j.jmb.2021.166983
Edited by S. Koide

Abstract

Recombinant antibodies (Abs) against the SARS-CoV-2 virus hold promise for treatment of COVID-19 and high sensitivity and specific diagnostic assays. Here, we report engineering principles and realization of a Protein-fragment Complementation Assay (PCA) detector of SARS-CoV-2 antigen by coupling two Abs to complementary N- and C-terminal fragments of the reporter enzyme *Gaussia* luciferase (Gluc). Both Abs display comparably high affinities for distinct epitopes of viral Spike (S)-protein trimers. Gluc activity is reconstituted when the Abs are simultaneously bound to S-protein bringing the Ab-fused N- and C-terminal fragments close enough together (8 nm) to fold. We thus achieve high specificity both by requirement of simultaneous binding of the two Abs to the S-protein and also, in a steric configuration in which the two Gluc complementary fragments can fold and thus reconstitute catalytic activity. Gluc activity can also be reconstituted with virus-like particles that express surface S-protein with detectable signal over background within 5 min of incubation. Design principles presented here can be readily applied to develop reporters to virtually any protein with sufficient available structural details. Thus, our results present a general framework to develop reporter assays for COVID-19, and the strategy can be readily deployed in response to existing and future pathogenic threats and other diseases.

Introduction

The recent approvals of highly effective vaccines against SARS-CoV-2 spells the likely endgame of worldwide efforts to eliminate the COVID-19 pandemic. Nonetheless, ongoing public health campaigns will remain essential to minimizing infection and mortality over the coming months, including testing and contact-tracing efforts. In this regard, simple, rapid and highly accurate point-of-care and field tests for SARS-CoV-2 remain a challenge now and for future pandemics.

Existing RT-PCR tests remain the standard of highly specific, accurate and sensitive methods to detect the SARS-CoV-2 virus, but require specialized expertise, reagents and equipment not available in the field.[1–4] Furthermore, the duration of the assays combined with the need to transport and prepare samples in centralized testing labs,

mean that results are not available for hours to days, precluding their use, for instance, for testing airline passengers for infection. Variants of PCR and CRISPR/Cas9-based tests have been developed that are rapid and simple to implement in the field but can have high false-negative rates.[2]

Serological tests can be used to detect the existence of natural neutralizing antibodies (Abs) against viral antigens in the blood of recovering or recovered virus-infected patients but cannot be used in the early stages of infection prior to mounting of an immune response.

Antigen-directed diagnostics that detect the SARS-CoV-2 spike (S-)protein have now been reported based on various technologies, including antibody-based field-effect transistor (limit of detection (LOD): 2.4×10^2 copies/mL),[5] nanoplasmonic resonance (LOD: 3.7×10^2 virus particles/mL),[6] and electrochemical sensors (LOD: 4×10^3 virus particles/mL)[7] that now appear to be sufficiently sensitive for diagnosis. These reporters use, however, a single antibody (CR3022[8]) which are cross-reactive with SARS-CoV-1 S- protein and thus lack specificity.

The highly specific nature of Abs binding to viral antigens does, however, suggest a strategy to use Abs as a component of reporters for virus in human samples. The challenge is to couple the binding of Abs to viral antigens directly to a simple and sensitive reporter assay. Furthermore, both specificity and sensitivity of such a reporter assay would be enhanced if multiple Abs that bind to different epitopes of viral protein antigens could be simultaneously coupled to the reporter. Finally, specificity would be further enhanced if one could link the structural-steric requirements for binding of multiple Abs to viral antigens to the function of the reporter assay. Here we describe a reporter assay for the SARS-CoV-2 virus surface-associated S-protein that meets these criteria, based on the binding of two recombinant Abs, which bind simultaneously to two unique epitopes on the S-protein. The two Abs are coupled to an enzymatic luminescence enzyme reporter Protein-fragment Complementation Assay (PCA) in which complementary N- and C-terminal fragments of the reporter enzyme are fused to one of the two Abs, respectively (Figure 1). Binding of the two Abs to the S-protein could bring the two complementary fragments of the reporter together in space where they can fold into active enzyme.[9] The steric requirements that the fragments be close enough in space are thus combined with the exquisite specificity of the Abs, resulting in a highly specific reporter system. Furthermore, the high sensitivity arising from the low signal to background of luminescent enzyme reporter assays assures a highly specific viral reporter. Finally, the assay should be simple to implement anywhere, requiring no specialized knowledge.

SARS-CoV-2 Abs that bind directly to the virus and inhibit entry into host cells have therapeutic potential. We have applied *in vitro* selections with phage-displayed libraries to construct synthetic Abs built on a single human framework derived from the highly validated drug trastuzumab. This approach has enabled the rapid production of high affinity Abs with properties optimized for drug development. Recombinant Abs that inhibit the interaction between SARS-CoV-2 and host cells confer protection in cell-based assays and animal models,[10,11] and efficacy has also been observed for Abs targeting the related coronaviruses SARS-CoV[12–14] and MERS.[15] Consequently, a number of Abs have entered clinical trials as post-infection treatment of COVID-19 associated with SARS-CoV-2 (Clinicaltrials.gov - NCT04452318, NCT04497987). We could select among the recombinant Abs that we have developed for therapeutic applications and apply these to develop a SARS-CoV-2 reporter. In particular we chose a pair of Abs that we could demonstrate bound to two unique epitopes of a SARS-CoV-2 surface antigen and for which structural models of the two nAb-antigen complexes were known, specifically of antibodies to the viral surface S-protein (Figure 1).

SARS-CoV-2 virions contain 25–100 glycosylated S-proteins that protrude from the virus surface.[16,17] Surface-associated S-proteins bind to angiotensin-converting enzyme 2 (ACE2) to mediate host cell entry.[18] The S-protein contains two subunits (S1 and S2) and forms a homotrimer. The receptor binding domain (RBD), located in the C-terminal region of the S1 subunit, recognizes ACE2 on host cells; binding facilitates cleavage of the S2 subunit by cell-surface proteases, which in turn promotes fusion and internalization of the virus.[18] The most potent Abs against both SARS-CoV-2 and SARS-CoV block ACE2 through direct competition for binding to the RBD.[19–23] Consequently, we have focused our efforts on developing Abs that bind to the RBD and compete with ACE2.

For the PCA reporter we chose the humanized *Gaussia princeps* luciferase (Gluc). This luciferase is among a family of homologous enzymes that are the smallest and have been shown to have the highest activity among reported luciferases.[24–26] Efforts to optimize the activity of Gluc and related luciferases has resulted in enzymes with activities detectable down to as low as attomole levels.[27] We have developed a PCA based on Gluc that has been widely used in a variety of applications to both *in situ* cellular and *in vitro* applications.[26] We have also shown that the PCA is reversible; that is, folding of the enzyme into its three-dimensional structure reverses completely on dissociation of protein complexes and consequently, the PCA is not a thermodynamic trap, which could lead to

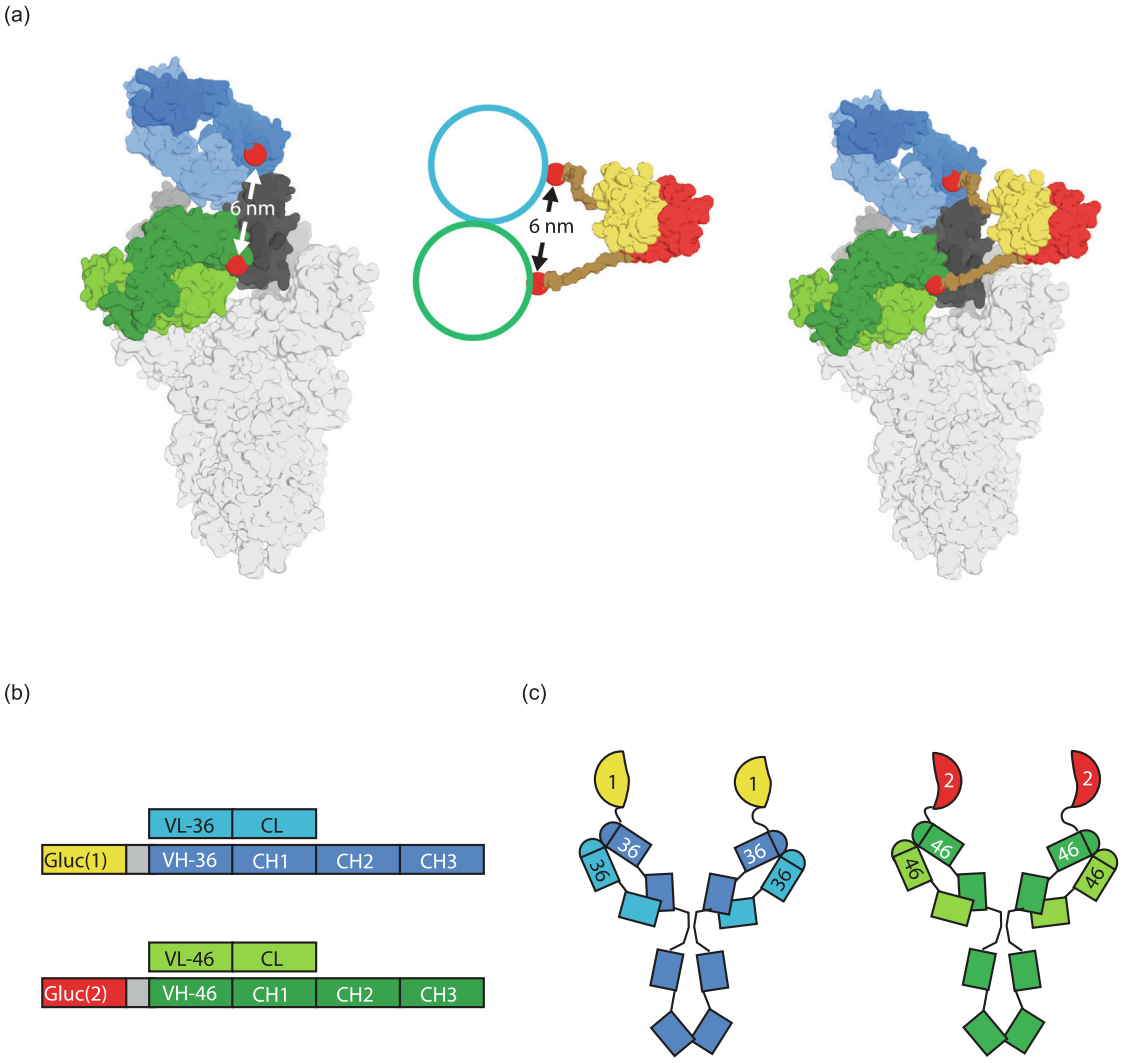

Figure 1. Structure based design of SARS-CoV-2 Gluc PCA. (a) (left panel) Structural model of the trimeric-spike of SARS-CoV-2 with the three receptor binding domains (RBD) represented in the "up" position based on the coordinates of PDB ID:6VBD. SARS-CoV-2 trimeric spike surface representation (white), with three RBDs (highlighted in different shades of gray) in the "up" position as described by Wilson *et al.*[8] One RBD is shown in complex with two antibody fragments (Fabs) with non-overlapping epitopes. The first Fab, with its light and heavy chain colored in light and dark blue, respectively, was modeled based on the crystal structure of 15033-7/SARS-CoV-2-RBD complex [PDB:7KLH]. The second Fab with its light and heavy chain colored in light and dark green, respectively, was modeled based on the crystal structure of CR3022/SARS-CoV-2-RBD complex (PDB ID: 6W41). Gluc fragments were modeled based on the coordinates of a protein of a similar size as Gluc (PDB ID: 4RZ9). Fragments 1–94 and 95–178 are colored in yellow and red, respectively. The linkers (brown) were modeled in, based on geometrical constraints. In the center panel, the two circles symbolize the location of the two proteins that would interact to bring the Gluc fragments close enough to reconstitute Gluc activity. The C-termini of the two chains are represented as red-colored spheres. The combination of steric constraints of geometry of the two Fabs interactions with an RBD (left panel) and distance constraints for reconstituting Gluc from its fragments (middle panel), results in prediction of the optimal assay configuration (right panel), where the Gluc fragments are fused to the N-termini of the heavy chains of the IgGs of the two complete antibodies, connected by 15 amino acid linkers (b and c). These models were generated on PyMol version 2.4. and the schematic representations of the Gluc-Fab fusion proteins were designed based on the structural analysis.

false-positive amplification of non-specific protein–protein interactions.[9]

We describe here the design and implementation of an S-protein-specific two-epitope Abs-Gluc PCA reporter for SARS-CoV-2 viruses.

Results

Structural analysis of the SARS-CoV-2 epitopes for PCA feasibility

Previous studies have shown that the SARS-CoV-2 RBD possesses at least 2 unique and non-overlapping epitopes within close proximity[8,28] suggesting the feasibility of a sensitive PCA that could improve COVID-19 diagnostics via detection of viral proteins rather than cDNA. Superposition of the Fab-RBD complexes for both structures (PDB:6W41 and PDB:7KLH) revealed no steric clashes between bound antibodies suggesting that they could bind the RBD simultaneously. Further analysis revealed that when co-complexed, the distance between the N-termini of the heavy chains of each antibody was 6 nm from one another (Figure 1(a), left-side panel). This distance is within the range of distances that could be bridged by 8 or more amino acid peptide linkers ($8 \times 2 \times 4$ Å = 6.4 nm) to enable reconstitution of an enzymatically active Gluc (Figure 1(a), centre panel). Empirically, we've found the best linker lengths for maximal reconstitution of PCA activities to be between 10 to 15 amino acids.[9]

These observations were extrapolated to the trimer SARS-CoV-2 S-protein, based on the cryo-electron microscopy model (PDB:6VSB). The three RBDs were placed in the up position and slightly rotated as described[8] to accommodate binding of CR3220 Fab. Based on this model, at least one of the three RBDs can be bound simultaneously by the antibody pair and bringing the two Gluc fragments in close enough proximity for folding and reconstitution of the luciferase activity, as illustrated in Figure 1(a), right panel. While Fabs were used in the structural modeling, we actually fused the Gluc fragments to full IgG molecules (Figure 1(b) and (c)), because the Fc portion of the IgG provides stability, solubility, and avidity advantages.

Identification of antibodies for development of the SARS-CoV-2 reporter PCA

Details of Fab and IgG engineering and structure determination of IgG-S-protein complexes were described previously.[28] Briefly, antibodies were selected from a phage-displayed human antigen-binding fragment (Fab) library, similar to the highly validated library F,[29] in multiple rounds of selection for binding to the RBD of the S-protein of SARS-CoV-2. Screening of Fab-phage clones for binding to the trimeric S-protein, revealed numerous clones whose epitope strongly overlapped with the host receptor, and these were converted into full-length human IgG1 format for purification and functional characterization.

To screen for candidate antibodies that could bind the SARS-CoV-2 RBD simultaneously, we conducted Fab-phage competition ELISAs against immobilized trimeric S-protein. Fab-phage for two well-characterized epitopes - one centred on the ACE2-binding site (15033[28]) and the other on a conserved epitope remote from the ACE2-binding site (CR3022[8]) were also included as controls to aid characterization. Results revealed two antibodies that at saturating concentration (250 nM) of IgG effectively self-blocked their own Fab-phage analog, one of which partially blocked Fab-phage 15033 (IgG 15036) and the other which blocked Fab-phage CR3022 (IgG 15046). Neither of these Abs blocked one another, confirming that they bound distinct epitopes and could thus, simultaneously bind to the S-protein RBD (Figure 2(a)).

To determine their apparent affinities, IgGs for 15036 and 15046 were assessed by direct binding ELISA to estimate EC_{50} values and biolayer interferometry (BLI) to determine binding kinetics. These results revealed dose-dependent and saturable binding to the S-protein in ELISA with estimated EC_{50} of 0.5 ± 0.1 nM and 1.3 ± 0.3 nM for IgG's 15036 and 15046, respectively (Figure 2(b)). Assessment of the binding of serial dilutions of each antibody to sensor-immobilized S-protein by BLI confirmed the tight binding to the homotrimer with $K_{D\ app}$ values of 0.1 ± 0.1 and 2.3 ± 0.6 nM for IgGs 15036 and 15046, respectively (Figure 2(c), S1). The binding of each antibody to the purified SARS-CoV-2 RBD were, however, identical ($K_{D\ app}$ = 2.2 ± 0.2 *versus* 3.7 ± 0.1 nM, respectively) and further, while no binding of IgG 15036 could be observed, IgG 15046 bound to the earlier SARS-CoV strain RBD with a similar apparent affinity of 2.2 ± 0.2 nM. These observations corroborate the phage competition results and confirms that IgG 15046 binds to an epitope that is conserved between the two viruses, while distinct from the epitope targeted by IgG 15036 and thus suitable for development of a PCA reporter.

Antibody-Gluc fusions for SARS-CoV-2 antigen detection

We ensured that the Gluc fragment addition as well as the mildly reducing conditions used for the Gluc activity reconstitution did not interfere with the binding of the antibody to SARS-CoV-2 RBD (Figure S2). To determine whether our reporter could work as a specific reporter of native SARS-CoV-2 viruses, we assessed how the Gluc-antibody fusion pairs reconstituted Gluc enzymatic activity specifically in the presence of SARS-CoV-2 S-protein by incubating 50 nM antibody fusion proteins with virus-like particles (VLPs) pseudotyped with and displaying SARS-CoV-2 S-protein on their surfaces, both at 10^9 particles per

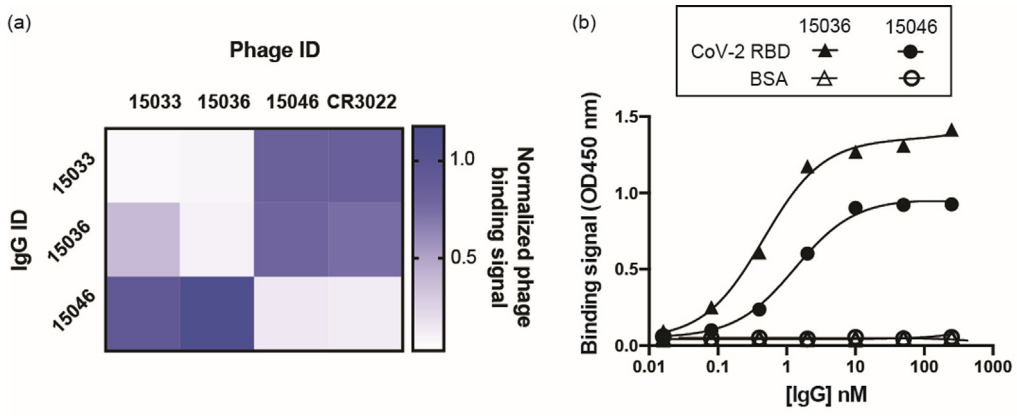

(c)

ID	Antigen	K_D (nM)	k_{on} ($10^5 s^{-1}$)	k_{off} ($10^{-5} M^{-1} s^{-1}$)
15036	CoV-1 RBD	NBD	NBD	NBD
	CoV-2 RBD	2.2 ± 0.2	10 ± 1.0	220 ± 4.6
	CoV-2 S-protein	0.1 ± 0.1	9.9 ± 0.1	12 ± 0.2
15046	CoV-1 RBD	2.2 ± 0.2	0.4 ± 0.1	9.2 ± 0.6
	CoV-2 RBD	3.7 ± 0.1	2.9 ± 0.1	110 ± 1.5
	CoV-2 S-protein	2.3 ± 0.6	1.9 ± 0.1	44 ± 1.0

Figure 2. Characterization of a candidate pair of antibodies for binding to distinct epitopes of SARS CoV-2 (CoV-2) RBD (a) A heat map to illustrate mapping of the relative binding to different epitopes of the candidate antibody pair by Fab-phage *versus* IgG competition ELISA. Binding signal of Fab-phage clones (x-axis) to immobilized S-protein assessed following pre-incubation with spike binding IgG (y-axis) and normalized to Fab-phage binding in the presence of a non-binding control antibody. (b) IgG binding to immobilized S-protein trimer or BSA control protein assessed by ELISA over a range of serial five-fold dilutions from 250 nM. (c) Binding kinetics for a candidate pair of RBD-binding antibodies with non-overlapping epitopes *versus* sensor-immobilized SARS-CoV-2 (CoV-2) S-protein and RBD and SARS-CoV-1 (CoV-1) RBD.

millilitre. Non-pseudotyped VLPs were used as a negative control to assess the level of non-specific Gluc activity. An incubation as short as 5 min lead to a significant luminescence signal 4 times greater for the SARS-CoV-2 pseudovirus than the control pseudovirus ($P < 0.03$) (Figure 3(a), left). We further monitored Gluc activity for up to 148 min achieving a highly significant 10 times greater signal for the SARS-CoV-2-pseudovirus *versus* the control pseudovirus ($P < 0.0001$) (Figure 3(a), right). To assess the specificity of our reporter, we compared its activity to that for SARS-CoV-1 S-protein. We observed significant activity for SARS-CoV-2 spike protein ($P < 0.004$) over background luminescence but no significant activity for SARS-CoV-1 S-protein ($P > 0.38$) (Figure 3(b)). These results demonstrate the potential of our reporter to specifically detect SARS-CoV-2 viruses.

Discussion

Our aim here was to apply protein engineering principles to develop a proof of concept for a specific, rapid and simple SARS-CoV-2 reporter assay. Virus-like particles pseudo-typed with SARS-CoV-2 S-protein are a widely used approximation of authentic virus that enables analysis outside of a biosafety level 3 facility. However, until direct comparison can be made, it is difficult to determine how the performance of this PCA on authentic viral particles would differ from that with the pseudovirus. Structural studies have confirmed that both arms of an IgG can simultaneously bind to adjacent RBDs on a trimeric spike and thus, in using IgG rather than Fab, we aimed to take advantage of the avidity effects of a bivalent antibody to achieve sufficient sensitivity for detection. On the surface of authentic virus, S-protein nearest neighbour distances can range from 10 to 50 nm, averaging 24 nm[16] and since the maximum inter-paratope distance of an IgG is about 1.5 nm, it is unlikely that Fab arms of a single antibody could bind adjacent S-proteins, the pseudovirus is not expected to differ in this regard. Furthermore, differences in S-protein sites, compositions and branching patterns of glycosylation may differ in cells in which authentic or pseudoviruses are produced could differ, resulting in hiding or revealing of epitopes or steric effects that could alter reporter sensitivity.

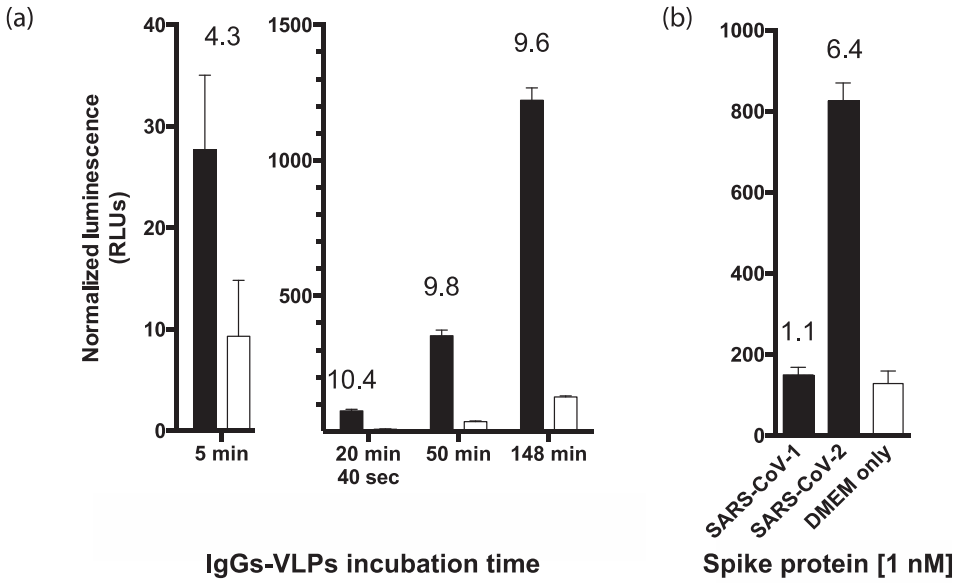

Figure 3. (a) Reconstitution of Gluc-IgG fusion activity by SARS-CoV-2 pseudotyped VLPs The luminescence (left y-axis) of IgG_{15036}-Gluc(1) and IgG_{15046}-Gluc(2) incubated with 10^9 per mL SARS-CoV-2 pseudotyped VLPs (expressing S-protein) (black bars) or control VLPs (without S-protein expressed) (white bars). A significant increase in activity (4.3 times) was observed for SARS-CoV-2 *versus* VLP control after 5 min (left panel) with increasing signal up to 148 min (right panel). (b) Reconstitution of Gluc-IgG fusion activity by the spike protein of SARS-CoV-2 but not the one of SARS-CoV-1. The luminescence (left y-axis) of IgG_{15036}-Gluc(1) and IgG_{15046}-Gluc(2) incubated for 50 min with 1 nM of spike protein of SARS-CoV-1, SARS-CoV-2, (black bars) or DMEM buffer (white bar) was measured. Significant increase in activity (6.4 times) was observed with SARS-CoV-2 but not with SARS-CoV-1 (1.1 fold) *versus* the control experiment.

Our reporter inherently relies on the binding of two antibodies to the target antigen. This provides a high level of specificity, as exemplified by the fact that even though one of the antibodies, 15046, binds to both SARS-CoV-1 and SARS-CoV-2 (Figure 2(c)), the reporter has strict specificity for SARS-CoV-2 (Figure 3(b)). This is due to the specificity of 15036 for SARS-CoV-2 (Figure 2(c)). This feature is important to take into account in the context of emergent variant of SARS-CoV-2: the loss of binding of one of the antibodies to the virus would make the reporter unable to detect the virus particles. We are actively working on generating antibodies that cross-react with these variants and these next generation antibodies could be used instead or in combination with the antibodies currently used in our reporter.

Nevertheless, testing with clinical isolates and further improvements of the reporter remain, but methods to achieve increased performance of luciferase reporters are well documented.[24,25,27,30] At present, our reporter is sensitive to 10^9 virus particles per millilitre but we estimate that with existing strategies, we could increase sensitivity to 10^6 virus particles, comparable to the sensitivity of RT-PCR methods used for diagnosis of disease from throat swabs and sputum that are estimated to contain 10^4 to 10^7 virus particles/mL.[31] As one approach, protein engineering techniques and modularity principles can be used to enhance the apparent affinity of natural bivalent IgGs, including those to the S-protein RBD, up to 1000-fold.[28] Furthermore, methods to improve Gluc activity *in vitro* have been explored and could be applied here to improve activity up to 1000 times.[24,25,27,30] Notably, the Gluc structure has 5 disulfide bonds that must be correctly formed when Gluc folds from its fragments.[32] We are now exploring ways to adjust redox conditions that will maximize the formation of the correct disulfides during folding Gluc following fragment complementation. Alternatively, homologues of Gluc have higher or comparable activity and result in better PCA activity. A PCA has already been developed from one such homologue, although its reversibility has not been documented.[33]

COVID-19 has exposed the need for rapid diagnostics development to respond to viral outbreaks in real time, to prevent the global spread of viral pathogens to the point where a pandemic threatens the entire global community. Though beta coronaviruses causing previous outbreaks have been eradicated or largely contained, other coronaviruses (HCoVs NL63, OC43, HKU1 and 229E) are globally endemic in human populations and estimated to be responsible for 15–30% of common colds[36]. In light of this, specificity - the ability to detect SARS-CoV-2 against a background of related innocuous viruses, is critical. In evaluating the binding of the candidate fusion pair of antibodies against the RBD from both

SARS-CoV-2 and its most closely related SARS, the exclusive binding of IgG 15036 to the former confirmed a lack of cross-reactivity. Though the binding of IgG 15046 to a conserved epitope on the two RBDs suggests that it could bind to other related CoVs, a viable PCA, insofar as it requires two antibodies, would not reconstitute a functional hGluc without binding of the second antibody. Specificity is thus a feature of our assay, established through judicious choice of epitopes and while a broader establishment of specificity remains, PCA-based diagnostics possess clear potential to be highly specific.

Alternatively, it will be important that antibodies maintain binding to emerging variants of SARS-CoV-2 that have compromised the binding and efficacy of clinical antibodies[34,35]. Though all antibody-based diagnostics are vulnerable to mutational escape, recombinant antibodies offer exquisite control over the paratope and thus provide some recourse to rapidly modify and optimize existing antibodies via directed evolution techniques to retain specificity for any variant. This iteration of the PCA is currently being evaluated against emerging variants to characterize binding and assay characteristics.

As scientists and governments alike grapple with the likelihood of future outbreaks, molecular surveillance could be aided by rapid diagnostics employed in the field. It is well established that coronaviruses exist and circulate in animal reservoirs confirmed by the identification of diverse S-protein sequences.[37–39] An advantage of selecting antibodies from phage-displayed libraries is that they do not require *a priori* human infection, but rather can be generated from the recombinant expression of and selection upon S-protein RBDs. Using principles illustrated in this manuscript, it would then be feasible to develop a PCA for virtually any coronavirus based upon the availability of S-protein sequences that could aid in future surveillance efforts.

Methods and Materials

Antibodies

Anti-M13 HRP conjugated antibodies (27-9421-01, GE Healthcare) were used for detection of Fab-phage. Anti-kappa-HRP conjugated antibodies (A8592, Sigma) were used for detection of IgG. The CR3022 Fab-phage clone was assembled from published sequences and cloned into a phage display vector using standard molecular techniques.

Cells

E. coli CJ236 (New England Biolabs) cells were used to produce dU-ssDNA for site-directed mutagenesis. E. coli SS320 (Genentech) cells were used for antibody library preparation. E. coli Omnimax (Invitrogen) cells were used for phage elution and amplification during the library selection. Mammalian cells were maintained in humidified environments at 37 °C in 5% CO_2 in the indicated media. HEK293T (ATCC) were maintained at 37 °C in 5% CO_2 in DMEM containing 10% (vol/vol) FBS. Expi293F cells (ThermoFisher) were maintained at 37 °C in 8% CO_2 in Expi293F expression media (ThermoFisher).

Protein production and purification

Trimeric SARS-CoV-1 and SARS-CoV-2 S-proteins, ACE2 protein, and SARS-CoV-1 and SARS-CoV-2 RBDs were produced as described,[28] then further purified by size-exclusion chromatography. For the RBDs and ACE2, a Superdex 200 Increase (GE healthcare) column was used. For the spike ectodomain, a Superose 6 Increase (GE healthcare) column was used. Purified proteins were site-specifically biotinylated in a reaction with 200 μM biotin, 500 μM ATP, 500 μM $MgCl_2$, 30 μg/mL BirA, 0.1% (v/v) protease inhibitor cocktail and not more than 100 μM of the protein-AviTag substrate. The reactions were incubated at 30 °C for 2 h and biotinylated proteins then purified by size-exclusion chromatography.

Library construction and phage display selections

A naive, synthetic phage-displayed antibody library, similar to previous libraries,[29] was used to select for SARS-CoV-2-binding antibodies by panning against purified S-protein RBD as described.[28]

Enzyme-linked immunosorbent assays

To conduct ELISAs, plates were first coated by overnight incubation at 4 °C with a 2 μg/ml solution of neutravidin. After immobilization and removal of protein solution, coated plates were blocked with PBS, 0.2% BSA for 1 h and then biotinylated S-protein or RBD captured from a 20 nM solution by incubation for 15 min with shaking at RT. After washing 4X with PBS plus 0.05% Tween, phage or Ab was added and allowed to bind for 30 min. Plates were subsequently washed, incubated with an appropriate secondary antibody, and developed with TMB substrate as described.[38]

Ab production and purification

IgG and Glu-IgG fusions were produced in Expi293F cells (ThermoFisher) by transient transfection, mixing equivalent amounts of expression construct DNA encoding the heavy and light chains in OptiMem serum-free media (Gibco) before complexation with FectoPro (Polyplus Transfection) for 10 min. Complexed DNA complex was then added to Expi293F cells

and expressed for 5 days. Expressed Abs were purified using rProtein A Sepharose (GE Healthcare), then buffer exchanged into PBS and concentrated using Amicon Ultra-15 Centrifugal Filter devices (Millipore) before storage.

Biolayer interferometry

The binding kinetics and estimation of apparent affinity (K_D) of Ab binding to the S-protein were determined by BLI with an Octet HTX instrument (ForteBio) at 1000 rpm and 25 °C. Biotinylated S-protein was first captured on streptavidin biosensors from a 2 μg/mL solution to achieve a binding response of 0.4–0.6 nm and unoccupied sites were quenched with 100 μg/mL biotin. Abs were diluted with assay buffer (PBS, 1% BSA, 0.05% Tween 20) and an unrelated biotinylated protein of similar size was used as negative control. Following equilibration with assay buffer, loaded biosensors were dipped for 600 s into wells containing 3-fold serial dilutions of each Ab starting at 67 nM, and subsequently, were transferred for 600 s back into assay buffer. Binding response data were corrected by subtraction of response from a reference and were fitted with a 1:1 binding model using ForteBio's Octet Systems software 9.0.

Generation of pseudotyped VLPs

HEK-293 cells (ATCC) were used to generate virus-like particles as described[28] then harvested by collection from cell supernatant 48 h after transfection and filter sterilized (0.44 μm, Millipore Sigma, Cat. No. SLHA033SS). The total protein concentration of the pseudotyped VLPs was quantified by Bradford assay (Bio-Rad) and used to infer the number of particles per mL based on the correspondence empirically defined previously [40].

Construction of the Gluc-antibody fusions

DNA fragments (Figure S3) synthesized by gBlocks® (Integrated DNA Technologies) were cloned into a pSCSTa mammalian expression vector linearized via digestion with *XbaI* and *NotI* restriction enzymes (New England Biolabs) using Gibson assembly (New England Biolabs). The resultant expression constructs encoding Gluc(1) and Gluc(2) fused with a 15 amino-acid long linker to the N-terminus of the heavy chain of 15036 and 15046 antibodies, respectively, were sequence validated and are as shown in Figure S3. The sequences of the variable light and heavy chains of the two antibodies are shown in Figure S3(c)–(f).

Production of the Gluc-antibody fusions and luminescence assay

Purified proteins were produced as described for antibody production with the exception of the buffer exchange which was done with PD MiniTrap G-25 desalting columns (GE Healthcare). Proteins were quantified by measuring 280-nm light absorbance and an *in vitro* luciferase assay was performed at final concentrations of 50 nM of purified protein per sample in a final volume of 50 μL of Dulbecco's Modified Eagle's Medium (DMEM) without phenol red (Sigma Aldrich). Purified proteins were first diluted into DMEM without phenol red containing 100 μM of DL-dithiothreitol (Sigma) and incubated for 2 hrs at room temperature, then one of the two antibody fusion were added to the assay plate (white polystyrene 96-well half area microplate, Corning), followed by the pseudotyped or control VLP, and finally the second antibody fusion. The mixture was mixed by pipetting the volume 5 times and incubated as indicated in the relevant experiment. Native coelenterazine (CTZ-SOL-in vitro, Nanolight Technology) was diluted in DMEM without phenol red for injection (injection volume: 50 μL) and assays performed at a final concentration of coelenterazine of 50 μM. Signal intensities (integrated over 20 s, with an injection delay of 1 s, and a gain set to 150) were read on a BioTek Synergy™ NEO plate-reader.

CRediT authorship contribution statement

Frederic A. Fellouse: Conceptualization, Methodology, Validation, Formal analysis, Investigation, Writing - original draft, Writing - review & editing, Visualization. **Shane Miersch:** Investigation, Writing - original draft, Writing - review & editing. **Chao Chen:** Investigation. **Stephen W. Michnick:** Conceptualization, Writing - original draft, Writing - review & editing, Supervision, Project administration, Funding acquisition.

DECLARATION OF COMPETING INTEREST

The authors declare that they have no known competing financial interests or personal relationships that could have appeared to influence the work reported in this paper.

Appendix A. Supplementary data

Supplementary data to this article can be found online at https://doi.org/10.1016/j.jmb.2021.166983.

Received 29 January 2021;
Accepted 31 March 2021;
Available online 08 April 2021

Keywords:
recombinant antibodies;
SARS CoV-2;
spike (S) protein;

protein-fragment complementation assay; Gaussia Luciferase

References

1. Vandenberg, O., Martiny, D., Rochas, O., van Belkum, A., Kozlakidis, Z., (2020). Considerations for diagnostic COVID-19 tests. *Nature Rev. Microbiol.*,. https://doi.org/10.1038/s41579-020-00461-z.
2. Shuren, J., Stenzel, T., (2020). Covid-19 molecular diagnostic testing - lessons learned. *N. Engl. J. Med.*, **383**, https://doi.org/10.1056/NEJMp2023830 e97.
3. Venter, M., Richter, K., (2020). Towards effective diagnostic assays for COVID-19: a review. *J. Clin. Pathol.*, **73**, 370–377. https://doi.org/10.1136/jclinpath-2020-206685.
4. Giri, B., Pandey, S., Shrestha, R., Pokharel, K., Ligler, F.S., Neupane, B.B., (2021). Review of analytical performance of COVID-19 detection methods. *Anal. Bioanal. Chem.*, **413**, 35–48. https://doi.org/10.1007/s00216-020-02889-x.
5. Seo, G., Lee, G., Kim, M.J., Baek, S.H., Choi, M., Ku, K.B., Lee, C.S., Jun, S., et al., (2020). Rapid detection of COVID-19 causative virus (SARS-CoV-2) in human nasopharyngeal swab specimens using field-effect transistor-based biosensor. *ACS Nano*, **14**, 5135–5142. https://doi.org/10.1021/acsnano.0c02823.
6. Huang, L., Ding, L., Zhou, J., Chen, S., Chen, F., Zhao, C., Xu, J., Hu, W., et al., (2021). One-step rapid quantification of SARS-CoV-2 virus particles via low-cost nanoplasmonic sensors in generic microplate reader and point-of-care device. *Biosens. Bioelectron.*, **171** https://doi.org/10.1016/j.bios.2020.112685.
7. Yousefi, H., Mahmud, A., Chang, D., Das, J., Gomis, S., Chen, J.B., Wang, H., Been, T., et al., (2021). Detection of SARS-CoV-2 viral particles using direct, reagent-free electrochemical sensing. *J. Am. Chem. Soc.*, **143** https://doi.org/10.1021/jacs.0c10810.
8. Yuan, M., Wu, N.C., Zhu, X., Lee, C.C.D., So, R.T.Y., Lv, H., Mok, C.K.P., Wilson, I.A., (2020). A highly conserved cryptic epitope in the receptor binding domains of SARS-CoV-2 and SARS-CoV. *Science (80-)*, **368**, 630–633. https://doi.org/10.1126/science.abb7269.
9. Michnick, S.W., Ear, P.H., Manderson, E.N., Remy, I., Stefan, E., (2007). Universal strategies in research and drug discovery based on protein-fragment complementation assays. *Nature Rev. Drug Discov.*, **6**, 569–582.
10. Alsoussi, W.B., Turner, J.S., Case, J.B., Zhao, H., Schmitz, A.J., Zhou, J.Q., Chen, R.E., Lei, T., et al., (2020). A potently neutralizing antibody protects mice against SARS-CoV-2 Infection. *J. Immunol.*, **205**, 915–922. https://doi.org/10.4049/jimmunol.2000583.
11. Shi, R., Shan, C., Duan, X., Chen, Z., Liu, P., Song, J., Song, T., Bi, X., et al., (2020). A human neutralizing antibody targets the receptor-binding site of SARS-CoV-2. *Nature*, **584**, 120–124. https://doi.org/10.1038/s41586-020-2381-y.
12. Sui, J., Li, W., Murakami, A., Tamin, A., Matthews, L.J., Wong, S.K., Moore, M.J., Tallarico, A.S.C., et al., (2004). Potent neutralization of severe acute respiratory syndrome (SARS) coronavirus by a human mAb to S1 protein that blocks receptor association. *Proc. Natl. Acad. Sci. USA*, **101**, 2536–2541. https://doi.org/10.1073/pnas.0307140101.
13. Zhu, Z., Chakraborti, S., He, Y., Roberts, A., Sheahan, T., Xiao, D., Hensley, L.E., Prabakaran, P., et al., (2007). Potent cross-reactive neutralization of SARS coronavirus isolates by human monoclonal antibodies. *Proc. Natl. Acad. Sci. USA*, **104**, 12123–12128. https://doi.org/10.1073/pnas.0701000104.
14. Ter Meulen, J., Bakker, A.B.H., Van Den Brink, E.N., Weverling, G.J., Martina, B.E.E., Haagmans, B.L., Kuiken, T., De Kruif, J., et al., (2004). Human monoclonal antibody as prophylaxis for SARS coronavirus infection in ferrets. *Lancet*, **363**, 2139–2141. https://doi.org/10.1016/S0140-6736(04)16506-9.
15. Corti, D., Zhao, J., Pedotti, M., Simonelli, L., Agnihothram, S., Fett, C., Fernandez-Rodriguez, B., Foglierini, M., et al., (2015). Prophylactic and postexposure efficacy of a potent human monoclonal antibody against MERS coronavirus. *Proc. Natl. Acad. Sci. USA*, **112**, 10473–10478. https://doi.org/10.1073/pnas.1510199112.
16. Klein, S., Cortese, M., Winter, S.L., Wachsmuth-Melm, M., Neufeldt, C.J., Cerikan, B., et al., (2020). SARS-CoV-2 structure and replication characterized by in situ cryo-electron tomography. *Nature Commun.*, **11**, 5885.
17. Ke, Z., Oton, J., Qu, K., Cortese, M., Zila, V., McKeane, L., Nakane, T., Zivanov, J., et al., (2020). Structures and distributions of SARS-CoV-2 spike proteins on intact virions. *Nature*,, 1–7. https://doi.org/10.1038/s41586-020-2665-2.
18. Hoffmann, M., Kleine-Weber, H., Schroeder, S., Mü, M.A., Drosten, C., Pö, S., (2020). SARS-CoV-2 cell entry depends on ACE2 and TMPRSS2 and is blocked by a clinically proven protease inhibitor. *Cell*, **181**, 271–280.e8. https://doi.org/10.1016/j.cell.2020.02.052.
19. Hansen, J., Baum, A., Pascal, K.E., Russo, V., Giordano, S., Wloga, E., Fulton, B.O., Yan, Y., et al., (2020). Studies in humanized mice and convalescent humans yield a SARS-CoV-2 antibody cocktail. *Science*, **369**, 1010–1014. https://doi.org/10.1126/science.abd0827.
20. Pinto, D., Park, Y.-J., Beltramello, M., Walls, A.C., Tortorici, M.A., Bianchi, S., Jaconi, S., Culap, K., et al. (n.d.) Cross-neutralization of SARS-CoV-2 by a human monoclonal SARS-CoV antibody. https://doi.org/10.1038/s41586-020.
21. Cao, Y., Su, B., Guo, X., Sun, W., Deng, Y., Bao, L., Zhu, Q., Zhang, X., et al., (2020). Potent neutralizing antibodies against SARS-CoV-2 identified by high-throughput single-cell sequencing of convalescent patients' B cells 73-84.e16 *Cell*, **182** https://doi.org/10.1016/j.cell.2020.05.025.
22. Rogers, T.F., Zhao, F., Huang, D., Beutler, N., Burns, A., He, W.T., Limbo, O., Smith, C., et al., (2020). Isolation of potent SARS-CoV-2 neutralizing antibodies and protection from disease in a small animal model. *Science (80.-)*, **369**, 956–963. https://doi.org/10.1126/science.abc7520.
23. Wan, J., Xing, S., Ding, L., Wang, Y., Gu, C., Wu, Y., Rong, B., Li, C., et al., (2020). Human-IgG-neutralizing monoclonal antibodies block the SARS-CoV-2 infection. *Cell Rep.*, **32** https://doi.org/10.1016/j.celrep.2020.107918.
24. Markova, S.V., Larionova, M.D., Vysotski, E.S., (2019). Shining light on the secreted luciferases of marine copepods: current knowledge and applications. *Photochem. Photobiol.*, **95**, 705–721. https://doi.org/10.1111/php.13077.
25. Markova, S.V., Larionova, M.D., Burakova, L.P., Vysotski, E.S., (2015). The smallest natural high-active luciferase:

cloning and characterization of novel 16.5-kDa luciferase from copepod Metridia longa. *Biochem. Biophys. Res. Commun.*, **457**, 77–82. https://doi.org/10.1016/j.bbrc.2014.12.082.
26. Remy, I., Michnick, S.W., (2006). A highly sensitive protein-protein interaction assay based on Gaussia luciferase. *Nature Methods*, **3**, 977–979.
27. Verhaegent, M., Christopoulos, T.K., (2002). Recombinant Gaussia luciferase. Overexpression, purification, and analytical application of a bioluminescent reporter for DNA hybridization. *Anal Chem.*, **74**, 4378–4385. https://doi.org/10.1021/ac025742k.
28. Miersch, S., Li, Z., Saberianfar, R., Ustav, M., Brett Case, J., Blazer, L., Chen, C., Ye, W., et al., (2020). Tetravalent SARS-CoV-2 neutralizing antibodies show enhanced potency 1 and resistance to escape mutations 2020.10.31.362848 *BioRxiv*,. https://doi.org/10.1101/2020.10.31.362848.
29. Persson, H., Ye, W., Wernimont, A., Adams, J.J., Koide, A., Koide, S., Lam, R., Sidhu, S.S., (2013). CDR-H3 diversity is not required for antigen recognition by synthetic antibodies. *J. Mol. Biol.*, **425**, 803–811. https://doi.org/10.1016/j.jmb.2012.11.037.
30. Larionova, M.D., Markova, S.V., Vysotski, E.S., (2018). Bioluminescent and structural features of native folded Gaussia luciferase. *J. Photochem. Photobiol., B*, **183**, 309–317. https://doi.org/10.1016/j.jphotobiol.2018.04.050.
31. Kevadiya, B.D., Machhi, J., Herskovitz, J., Oleynikov, M.D., Blomberg, W.R., Bajwa, N., et al., (2021). Diagnostics for SARS-CoV-2 infections. *Nature Mater.*,.
32. Wu, N., Kobayashi, N., Tsuda, K., Unzai, S., Saotome, T., Kuroda, Y., Yamazaki, T., (2020). Solution structure of Gaussia Luciferase with five disulfide bonds and identification of a putative coelenterazine binding cavity by heteronuclear NMR. *Sci. Rep.*, **10**, 20069. https://doi.org/10.1038/s41598-020-76486-4.
33. Dixon, A.S., Schwinn, M.K., Hall, M.P., Zimmerman, K., Otto, P., Lubben, T.H., Butler, B.L., Binkowski, B.F., et al., (2016). NanoLuc complementation reporter optimized for accurate measurement of protein interactions in cells. *ACS Chem. Biol.*, **11**, 400–408. https://doi.org/10.1021/acschembio.5b00753.
34. Wang, P., Nair, M.S., Liu, L., Iketani, S., Luo, Y., Guo, Y., et al., (2021). Increased resistance of SARS-CoV-2 variants B.1.351 and B.1.1.7 to antibody neutralization. *bioRxiv*,.
35. Widera, M., Wilhelm, A., Hoehl, S., Pallas, C., Kohmer, N., Wolf, T., Rabenau, H.F., Corman, V., et al., (2021). Bamlanivimab does not neutralize two SARS-CoV-2 variants carrying E484K in vitro. *MedRxiv*,. https://doi.org/10.1101/2021.02.24.21252372.
36. Paules, C.I., Marston, H.D., Fauci, A.S., (2020). Coronavirus infections-more than just the common cold. *JAMA - J. Am. Med. Assoc.*, **323**, 707–708. https://doi.org/10.1001/jama.2020.0757.
37. Hu, B., Zeng, L.-P., Yang, X.-L., Ge, X.-Y., Zhang, W., Li, B., Xie, J.-Z., Shen, X.-R., et al., (2017). Discovery of a rich gene pool of bat SARS-related coronaviruses provides new insights into the origin of SARS coronavirus. *PLoS Pathog.*, **13**, https://doi.org/10.1371/journal.ppat.1006698 e1006698.
38. Lau, S.K.P., Woo, P.C.Y., Li, K.S.M., Huang, Y., Tsoi, H.W., Wong, B.H.L., Wong, S.S.Y., Leung, S.Y., et al., (2005). Severe acute respiratory syndrome coronavirus-like virus in Chinese horseshoe bats. *Proc. Natl. Acad. Sci. USA*, **102**, 14040–14045. https://doi.org/10.1073/pnas.0506735102.
39. Luk, H.K.H., Li, X., Fung, J., Lau, S.K.P., Woo, P.C.Y., (2019). Molecular epidemiology, evolution and phylogeny of SARS coronavirus. *Infect. Genet. Evol.*, **71**, 21–30. https://doi.org/10.1016/j.meegid.2019.03.001.
40. Steppert, P., Burgstaller, D., Klausberger, M., Tover, A., Berger, E., Jungbauer, A., (2017). Quantification and characterization of virus-like particles by size-exclusion chromatography and nanoparticle tracking analysis. *J. Chromatogr. A*, **1487**, 89–99. https://doi.org/10.1016/j.chroma.2016.12.085.